ISBN: 978-3-95450-231-8 ISSN: 2673-5490 doi: 10.18429/JACoW-IPAC2023-WEPL110

NONLINEAR DYNAMICS OF SCALING FFAS

M. Topp-Mugglestone*[1], S. Machida, J.-B. Lagrange, ISIS Department, RAL, STFC, UK
S. Sheehy, University of Melbourne, Victoria, Australia and ANSTO, Sydney, Australia
[1]also at John Adams Institute, University of Oxford, Oxford, UK

Abstract

Fixed Field Alternating Gradient Accelerators (FFAs) that follow the conventional scaling law have – by definition – high order multipole components in their magnetic fields. It is the presence of these nonlinearities that in many cases determines several important properties of the machine, including amplitude-dependent tune shift and dynamic aperture (DA). Consequently, understanding of the nonlinear dynamics in these machines can be critical to design and optimisation processes. Study of these properties is made challenging by the complicated nature of closed orbits in many FFAs and the presence of edge angle effects (which are exploited by design in certain lattice configurations, such as the F-D spiral design chosen as the baseline for the FETS-hFFA prototype ring). This poster presents numerical studies of the nonlinear properties of an FFA based on a harmonic analysis technique, with aim to improve understanding of the effects that limit the dynamic aperture and develop steps towards mitigating these factors.

INTRODUCTION

Fixed Field Alternating Gradient Accelerators (FFAs) present the opportunity for energy-efficient, high beam current operation, rendering them an attractive option for a number of future applications. In particular, the FETS-FFA proof of concept machine [1] aims to demonstrate the concept's viability as a high intensity proton driver for a spallation source complex.

In an FFA, time-independent DC magnetic fields are used in place of the ramped magnetic fields used by a synchrotron. The beam orbit is then permitted to move as a function of its energy. In a conventional, horizontal-excursion FFA, the orbit enlarges radially as energy increases. To maintain the machine's compactness, the field is then given a spatial dependence such that higher-energy particles tend to pass through stronger fields.

In particular, FFAs can be designed with a spatial field dependence such that a constant tune is maintained over their acceleration cycle by obeying a scaling law [2]. In the case of a horizontal-excursion FFA (hFFA) this can be satisfied if the field has a radial dependence as follows:

$$B(r) = B_0 \left(\frac{r}{r_0}\right)^k, \qquad (1)$$

in which r is the radial coordinate, B_0 represents a reference magnetic field specified at the radius r_0, and finally k is a parameter commonly known as the field index, to be specified by the machine's designer.

* max.topp-mugglestone@physics.ox.ac.uk

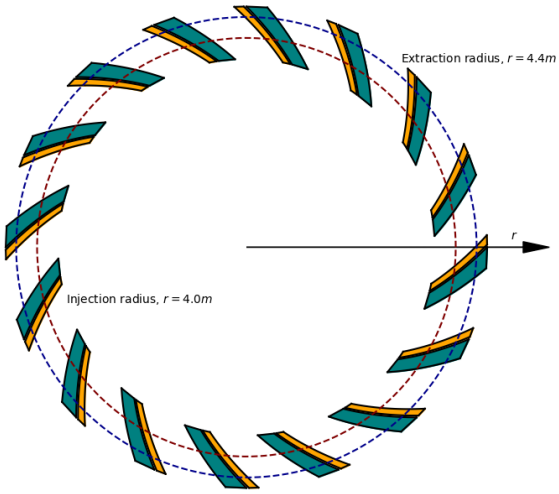

Figure 1: A plan view of the proposed FETS-FFA ring, a 16-cell 3-12MeV proton FFA based on an FD spiral lattice with a design tune of (3.41, 3.39). The regions shaded in teal represent the normal bend (F) magnets, and orange regions represent reverse bend (D) magnets.

In previously constructed FFAs, such as the 150 MeV proton machine at KURNS[3], radial sector magnets were used, and alternating gradient focussing was provided by the inclusion of reverse bend segments. However, if the vertical focussing can be enhanced through edge effects of the main magnets, the need for an opposite-polarity reverse bend section can be reduced, and the machine can be made more compact. This inspired the development of the spiral-sector FFA concept (Figure 1)[4], in which the mid-plane fields of the machine follow the form[5]:

$$B(r,\theta) = B_0 \left(\frac{r}{r_0}\right)^k \mathcal{F}\left[\tan\zeta \ln\frac{r}{r_0} - N\theta\right]. \qquad (2)$$

Here, θ represents the azimuthal coordinate, N is the periodicity of the ring, and ζ is a new design parameter that determines the spiral angle. The issue with increasing the spiral angle, however, is that the dynamic aperture (DA) of the machine is typically reduced with increased spiral angle. Understanding this effect is critical to optimise the design of a spiral-sector scaling FFA – particularly in high-intensity applications with significant space-charge effects.

METHOD OF HARMONIC ANALYSIS

When realistic fringe field models are included, determination of a closed orbit in such a machine has to rely on numerical integration techniques. This, on top of the highly

ISBN: 978-3-95450-231-8 ISSN: 2673-5490 doi: 10.18429/JACoW-IPAC2023-WEPL110

non-linear nature of the fields (which appear as a direct consequence of the scaling law, Equation 1) and the presence of edge-angle effects renders understanding of the high-order dynamics of the machine challenging in most applications. This section presents a method for the numerical study of the optical effects seen by a particle travelling through a lattice, taking into account the transformation into the Frenet-Serret frame.

A multi-step numerical procedure is followed to obtain a multipole decomposition of fields along the closed orbit:

1. Determine closed orbit using an optimisation routine in a numerical tracking code such as FIXFIELD [6]
2. For each integration step along the closed orbit, draw a circle of radius dr perpendicular to the instantaneous tangent vector of the closed orbit.
3. At each point along the circumference of this circle, measure the dot product of the local magnetic field with the radius vector of the circle to give the effective radial B-field.
4. Apply a Fourier transform to the radial magnetic fields around the circle.
5. Normalise Fourier series coefficients by dr^{n-1} (where n is the order of the coefficient) to obtain the local multipole series coefficients as a function of position along the closed orbit.

In certain cases (particularly in vertical-excursion FFAs [7, 8]) it is also necessary to measure the longitudinal fields (i.e. the dot product of the field on the closed orbit with the tangent vector of the closed orbit) to account for solenoid-type behaviour. This is always zero on the midplane of a hFFA, so need not be considered in the following analysis.

The dipole and quadrupole coefficients of such a decomposition can be used to set transfer matrix coefficients in a simple kick-drift integration code, and the accuracy of the composition tested by using this code to retrieve the tunes of the machine as measured in other codes.

AMPLITUDE-DEPENDENT TUNE SHIFT

The tune shift away from resonance for a perturbation potential V [9, 10] can be expressed as follows, making use of the smooth approximation:

$$\Delta\nu = \frac{1}{2\pi}\int_0^{2\pi} \frac{\partial\langle V\rangle}{\partial J} d\theta \tag{3}$$

in which $\langle\rangle$ denotes the double integral over the independent variable θ and the angle variable ϕ of the action-angle coordinate system, and J is the action variable of the system. The potential for a normal octupole with strength $k_3(\theta)$ can be expressed in action-angle coordinates as

$$V(\phi,\theta) = J^2 k_3(\theta)\beta^2(\theta)\sin^4\phi, \tag{4}$$

resulting in the tune shift

$$\Delta\nu = J\frac{3}{8\pi}\int_0^{2\pi} \beta^2(\theta)k_3(\theta)d\theta \tag{5}$$

In the above, k_3 is a coefficient that characterises the strength of the octupole perturbation. This can be expressed in terms of the octupole field adjusted for magnetic rigidity $B\rho$ as

$$B_y + iB_x = (k_3 B\rho)\,(x+iy)^3\,. \tag{6}$$

ANALYSIS

Lattices based on the design specifications of the FETS-FFA ring are generated. The model assumes an Enge function fringe field profile [11].

Here the spiral angle ζ is varied, and the horizontal and vertical tunes are kept constant by varying the B_0 of the reverse bend 'D-magnet' as well as the overall k-value of the lattice. Figure 2a shows the octupole strength (equal to $k_3 B\rho$, and expressed in units T/m^3) at each point along the orbit of a 3MeV proton beam, whilst Figure 2b displays the vertical beta functions on the same axis.

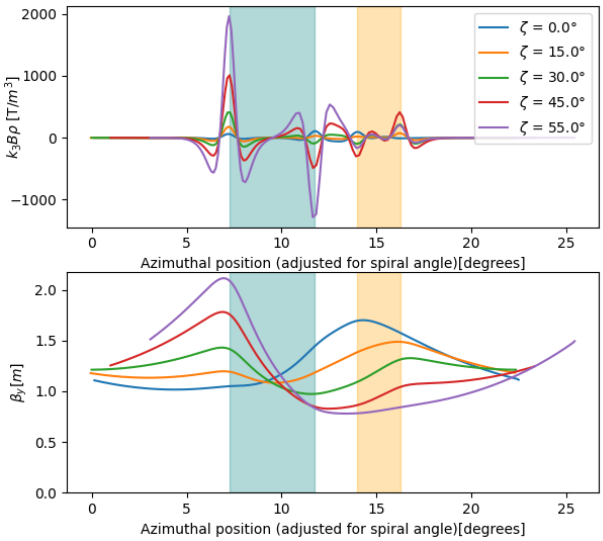

Figure 2: a). Octupole strength $k_3 B\rho$ throughout the cell in units T/m^3. The horizontal axis is the azimuthal coordinate along the closed orbit trajectory, generalised for the spiral angle by subtracting $\tan\zeta \ln\frac{r}{r_0}$ in which r is the radial coordinate of the trajectory at each point. The shaded teal region shows the position of the F-magnet, whilst the orange region shows the position of the D-magnet. All trajectories are computed for a proton beam at the 3MeV injection energy. b). Beta functions in units m plotted along the trajectories through the cell, using the same horizontal axis and shading scheme as above.

This shows that not only do particles see a greater octupole strength when the spiral angle is increased, but that the effect of this on the ultimate tune shift is further exacerbated by an increased beta function with spiral angle at this point. By

ISBN: 978-3-95450-231-8 ISSN: 2673-5490 doi: 10.18429/JACoW-IPAC2023-WEPL110

applying equation 5, the corresponding tune shifts can be computed; the result is shown in Figure 3b. Figure 3a shows how the B_d and k lattice parameters are varied to maintain a constant tune when the spiral angle is increased.

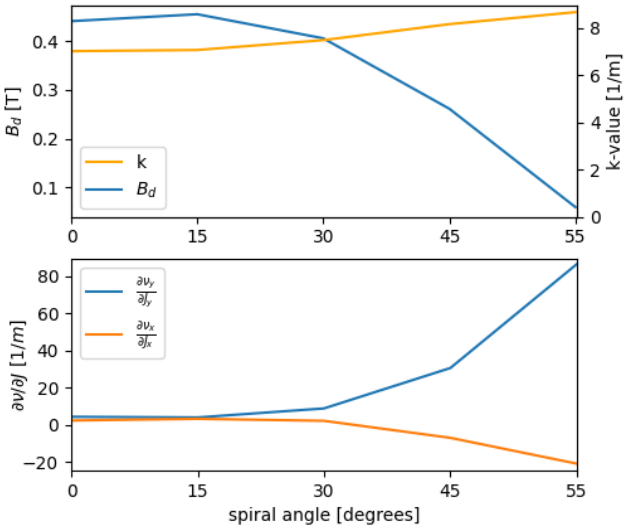

Figure 3: a). Dependence of lattice k-value (units 1/m) and reference B-field (units T) in the D-magnet on spiral angle. b). Horizontal (orange) and vertical (blue) amplitude-dependent tune shifts in the FETS-FFA lattice as a function of the spiral angle.

This shows that a spiral angle of 45 degrees is sufficient to reduce the required field strength of the D-magnet by approximately 50%. However, when the spiral angle is increased beyond this point, the amplitude dependent tune shift rises sharply as a consequence of the coincidentally increased octupole and beta function at the entrance of the F-magnet. This is a contributing factor to the reduction in dynamic aperture for large spiral angle as observed in tracking studies for the FETS ring [12].

The horizontal tune shift, by contrast, appears more stable as a function of the spiral angle. An explanation for this can be seen when we compare the beta function for the horizontal plane (Figure 4) to the previous plot of the octupole coefficient (Figure 2a).

As spiral angle is increased to 45 degrees, the horizontal beta function becomes larger at the position of the negative octupole component at the exit of the F-magnet. When the beta function and the octupole coefficients are multiplied, the negative octupole at the exit of the F-magnet is able to cancel the positive tune shift that would otherwise be induced by the positive octupole component at the F-magnet entrance. As the spiral angle is increased beyond 30 degrees, the drop in beta function at the location of the positive octupole causes the negative tune shift to become dominant and hence the total horizontal amplitude-dependent tune shift becomes negative for large spiral angles.

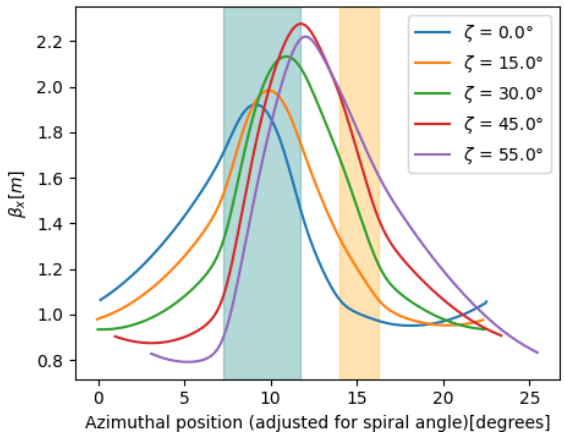

Figure 4: Horizontal beta function along the closed orbit of a cell as the spiral angle ζ is varied.

CONCLUSION

The method presented here can be used to give insight into the limiting factors on the dynamic aperture of complicated machines with closed orbits that are not known *a priori*. By applying this multipole decomposition along a closed orbit, it was possible to determine the leading sources of tune shift in the FETS-FFA lattice, and how these depend on key design parameters such as the spiral angle.

Implementation of this form of analysis into future study and optimisation procedures can enable an increased understanding of a machine and a more efficient design procedure. For example, the octupole and beta function product integral employed here can be used for a quick computation of the expected amplitude-dependent tune shift. This could be used to choose an optimal working point for the ring to avoid resonances, or to give a rapid estimate of DA for a given tune, which could be inserted into a numerical optimisation procedure and used to identify the best set of lattice parameters to maximise DA. In this application, this metric would be able to replace computationally intense particle survival simulations, enabling more streamlined optimisation processes and aiding in the design and study of future machines.

REFERENCES

[1] S. Machida *et al.*, "FFA Design Study for a High Intensity Proton Driver", presented at the IPAC'23, Venice, Italy, May 2023, paper TUPA044, this conference.

[2] A. A. Kolomensky, A.N. Lebedev, M. Barbier, and D. Keefe, "Theory of Cyclic Accelerators," *Physics Today*, vol. 20, no. 1, pp. 117–118, 1967. doi:10.1063/1.3034106

[3] T. Adachi *et al.*,"A 150MeV FFAG Synchrotron with Return-Yoke Free" Magnet"", in *Proc. PAC'01*, Chicago, IL, USA, Jun. 2001, paper RPPH016, pp. 3254–3256. doi:10.1109/PAC.2001.988075

ISBN: 978-3-95450-231-8 ISSN: 2673-5490 doi: 10.18429/JACoW-IPAC2023-WEPL110

[4] K. R. Symon, D.W. Kerst, L.W. Jones, L. J. Laslett, and K. M. Terwilliger, "Fixed-field alternating-gradient particle accelerators," *Phys. Rev.*, vol. 103, pp. 1837–1859, 1956. doi:10.1103/PhysRev.103.1837

[5] F. Meot, "RACCAM: An example of spiral sector scaling FFA technology," 2019, doi:10.2172/1507116

[6] J.-B. Lagrange, R. Appleby, J. Garland, J. Pasternak, and S. Tygier, "Racetrack FFAG muon decay ring for nuSTORM with triplet focusing," *J. Instrum.*, vol. 13, no. 09, p. P09013, 2018. doi:10.1088/1748-0221/13/09/P09013

[7] M. E. Topp-Mugglestone, J.-B. Lagrange, S. Machida, and S. L. Sheehy, "Studies of the Vertical Excursion Fixed Field Alternating Gradient Accelerator", in *Proc. IPAC'22*, Bangkok, Thailand, Jun. 2022, pp. 535–538. doi:10.18429/JACoW-IPAC2022-MOPOTK036

[8] M. Topp-Mugglestone, "Progress towards modelling of the vFFA," Workshop on Fixed Field Accelerators, 2022.

[9] M. Aiba *et al.*, "Study of Acceptance of FFAG Accelerator", in *Proc. EPAC'02*, Paris, France, Jun. 2002, paper WEPLE063, pp. 1226–1228.

[10] A.W. Chao, *Special Topics in Accelerator Physics*, World Scientific, 2022, p. 289. doi:10.1142/12757

[11] H. Enge, Deflecting magnets, in "Focusing of Charged. Particles", edited by A. Septier, 1967.

[12] S. Machida, "FFA study for ISIS-II and FETS-FFA," Workshop on Fixed Field Accelerators, 2022.